

May 2026

IEA Wind TCP Task 49

**The IEA Wind RFA1
Shallow-Water Reference
Floating Array Design**



iea wind

**Prepared for the
IEA Wind TCP**



May 2026

Authors:

Muk Chen Ong

Chern Fong Lee

University of Stavanger

Daniel Mulas Hernando

IEA Wind Task 49

Marek Jan Janocha

SINTEF Ocean AS

Ju Feng

Technical University of Denmark

IEA Wind TCP functions within a framework created by the International Energy Agency (IEA). Views, findings, and publications of IEA Wind do not necessarily represent the views or policies of the IEA Secretariat or of all its individual member countries. IEA Wind is part of IEA's Technology Collaboration Programme (TCP).

Acknowledgments

This report is a product of International Energy Agency Wind Technology Collaboration Programme (IEA Wind) Task 49 on Integrated Design of Floating Wind Arrays. The engagement of all participants in Task 49 Work Package 2 and additional review from other participants in Task 49 is gratefully acknowledged.

The contribution from the University of Stavanger (UiS) is funded by the Research Council of Norway (RCN) through ImpactWind SouthWest project (RCN project number 332034).

The contribution from the Technical University of Denmark (DTU) is funded by the Danish Energy Technology Development and Demonstration Program (EUDP) through the IDEA project under project number 134-21029.

List of Acronyms

ABS	American Bureau of Shipping
AEP	annual energy production
AHT	anchor handling tug
API	American Petroleum Institute
BOS	balance of system
CapEx	capital expenditures
CLV	cable lay vessel
CTV	crew transfer vessel
DLC	design load case
DSV	diving support vessel
FCR	fixed charge rate
FLORIS	FLOW Redirection and Induction in Steady State
GW	gigawatt
IEA	International Energy Agency
IEC	International Electrotechnical Commission
kg	kilogram
km	kilometer
kN	kilonewton
LCOE	levelized cost of energy
m	meter
MBL	minimum breaking load
MBR	minimum bending radius
mm	millimeter
MW	megawatt
MWh	megawatt-hour
N	newton
NLR	National Laboratory of the Rockies
O&M	operations and maintenance
OCS	Outer Continental Shelf
OpEx	operational expenditures
ORBIT	Offshore Renewables Balance-of-System and Installation Tool
OSS	offshore substation
POI	point of interconnection
TLP	tension-leg platform
USD	U.S. dollar
WAVES	Wind Asset Value Estimation System
WOMBAT	Windfarm Operations and Maintenance cost-Benefit Analysis Tool

Executive Summary

This report presents a reference floating wind array design for a shallow-water site developed under Task 49 of the IEA Wind Technology Collaboration Programme. It is the task's first reference floating array (RFA) produced for shallow water, and it is given the name IEA Wind RFA1. The design consists of a 1-GW floating wind farm composed of 67 IEA Wind 15-MW reference turbines supported by the University of Maine VoltturnUS-S semisubmersible platform. The floating array is designed based on the meteorological and oceanographic conditions of Sørlike Nordsjø II (SN2), Norway, with a representative water depth of 60 m. A semi-taut mooring system with suction anchors is adopted, while the dynamic cables employ lazy-wave configurations. The array layout follows a regular rectangular grid arrangement covering a total area of 345 km².

The mooring system is primarily composed of polyester rope with short chain segments at the anchor and fairlead connections. Compared with conventional chain-catenary systems typically used at similar water depths, the elasticity of the polyester rope provides a more linear restoring response. Clump weights are installed along the upper chain segments to compensate for the reduced system weight and mitigate large tension peaks, while subsea buoys are attached to the polyester segments to prevent seabed abrasion. Lazy-wave dynamic cable configurations of three conductor sizes are used within the reference design: 300, 630, and 1,000 mm². A key challenge in the cable design is maintaining the suspended configuration throughout the service life while satisfying allowable curvature and tension limits under extreme environmental loading conditions.

The wind farm adopts a uniform grid layout with equal spacing between adjacent rows and columns. Following the definition of the project boundary, the number of rows and columns is selected to maximize turbine spacing within the available area. The grid orientation is aligned with the geometry of the SN2 project area.

The cost and logistics assessment follows a transparent, open-source methodology and set of assumptions used to evaluate the shallow-water design, accounting especially for the effects of the mooring, cable, and layout design choices. The analysis combines process-based installation and O&M logistics models with wake-loss and AEP simulations to estimate project costs, energy generation, and the resulting LCOE. The LCOE for the 1-GW floating wind farm is estimated at \$138.01/MWh.

Overall, this report provides a baseline reference design and associated methodology to support future research and development of floating wind arrays in shallow-water environments. The corresponding input files and design documentation will be made publicly available through GitHub. In addition, the design description will follow the standardized Task 49 ontology format to facilitate data sharing, interoperability, and future collaborative research efforts.

Table of Contents

Executive Summary	v
1 Introduction	1
2 Site Conditions	3
3 Mooring Design	6
3.1 Design Assumptions and Requirements	6
3.2 Design Approach	7
3.3 Mooring Design Description	7
3.4 Performance Results	10
3.4.1 Mooring Line Tension	10
3.4.2 Rope Ground Contact	11
3.4.3 Maximum Horizontal Platform Displacement	12
3.4.4 Fatigue Analysis	13
4 Anchor Design	15
4.1 Design Assumptions and Requirements	15
4.2 Anchor Design Description	15
5 Dynamic Cable Design	17
5.1 Design Assumptions and Requirements	17
5.2 Design Approach	19
5.3 Dynamic Cable Design Descriptions	20
5.4 Performance Results	21
5.4.1 Cable Tensions	22
5.4.2 Cable Curvatures	23
5.4.3 Cable Ground Contact	24
6 Layout	26
7 Cost and Logistics Modelling	29
7.1 Methodology	29
7.2 Inputs and Assumptions	29
7.2.1 Plant Characteristics Summary	30
7.2.2 Task 49 Design Basis Cost and Logistics Considerations	31
7.3 Results 32	
7.3.1 FCR	32
7.3.2 CapEx	32
7.3.3 OpEx	34
7.3.4 Net AEP	34
7.3.5 LCOE	35
8 Conclusion	36
References	37

List of Figures

Figure 1. Location of SN2 [4].	3
Figure 2. Polar histograms of the mean wind speed at 150 m height, significant wave height (Hs) and spectral peak period (Tp) at SN2 [4].	4
Figure 3. Environment headings used for strength load cases	7
Figure 4. VoltturnUS-S platform and shallow-water mooring system	8
Figure 5. Line tension statistics.	10
Figure 6. Line tension maximum and minimum values.	11
Figure 7. Line 1 Vertical Elevation Envelope under DLC 6.1 at 0°.	11
Figure 8. Line 1 Vertical Elevation Envelope under DLC 6.1 at 180°.	12
Figure 9. Statistics of the platform horizontal displacement.	12
Figure 10. Mooring line orientation for fatigue analysis.	13
Figure 12. Suction anchor capacity.	15
Figure 13. Bend Stiffener Dimensions.	18
Figure 14. Cable Capacity Curves [18].	18
Figure 15. Numerical Boundary of the Parametric Optimization.	19
Figure 16. Dynamic Cable Orientation.	20
Figure 17. Hydrostatic Lazy-wave Cable Profiles.	21
Figure 18. Dynamic cable tension statistics at HOP and TDP.	22
Figure 19. Dynamic cable maximum tensions at HOP and TDP.	23
Figure 20. Dynamic cable curvature statistics at HOP and TDP.	23
Figure 21. Dynamic cable maximum curvatures at HOP and TDP.	24
Figure 22. Cable Vertical Displacement Envelope under DLC 6.1 at 0°.	24
Figure 23. Cable Vertical Displacement Envelope under DLC 6.1 at 180°.	25
Figure 24. Orientation of the layout grid.	26
Figure 25. Array layout and cable routing	27
Figure 26. SN2 site location. Distances from OSS to assumed POI and construction port shown are used for cost and logistic modelling.	30
Figure 27. LCOE waterfall in \$/MWh.	35

List of Tables

Table 1. Shallow-Water Design Specifications [1].....	1
Table 2. Metocean Parameters for Critical Strength Load Cases	5
Table 3. Current Profiles at Different Return Periods.....	5
Table 4. Marine Growth Thickness at Two Depth Ranges.....	5
Table 5. Mooring Design Criteria.....	6
Table 6. Mooring Design Parameters	9
Table 7. Mooring Line Properties Including Marine Growth.....	9
Table 8. Final Suction Anchor Configuration and Verification Summary	16
Table 9. Dynamic Cable Properties	17
Table 10. Buoyancy Module Properties.....	18
Table 11. Lazy-Wave Cable Design Parameters.....	20
Table 12. Cable Equivalent Properties With Marine Growth.....	21
Table 13. Array Layout and Mooring Line Orientation Parameters	27
Table 14. Turbine and Substation Coordinates.....	28
Table 15. Summary of Design Basis Considerations by Key LCOE Driver	31
Table 16. Cost and Mass of the Mooring System	31
Table 17. Cost and Mass of the Suction Anchor.....	31
Table 18. Cost and Mass of 66-kV Array Cables	32
Table 20. CapEx Breakdown in 2024 USD	33
Table 21. OpEx Breakdown in 2024 USD.....	34
Table 22. Breakdown of Losses from Gross to Net Generation	34

1 Introduction

International Energy Agency Wind Technology Collaboration Program (IEA Wind TCP) Task 49 aims to accelerate the sustainable commercialization of floating wind arrays through the development of open-access reference information and array designs. The task is organized into four core work packages, with Work Package 2 (WP2) focusing on the development of reference floating wind array configurations. To represent a range of site conditions, WP2 is divided into three subgroups responsible for developing array designs for shallow- (60 m), intermediate- (320 m), and deep-water (800 m) environments. The corresponding reference floating array (RFA) designs are labelled IEA Wind RFA1, RFA2, and RFA3. Starting from an existing floating offshore wind turbine (FOWT) concept, the scope of each subgroup is to develop the corresponding mooring system, dynamic cable, array layout, and cable routing for the respective water depth.

In this report, the IEA Wind RFA1 shallow-water reference design with a representative water depth of 60 m is presented. The selected mooring system adopts a semi-taut chain–polyester–chain configuration, while lazy-wave dynamic power cables are employed. An overview of the shallow-water design specifications is provided in Table 1. The reference array consists of a 1-GW floating wind farm comprising 67 IEA Wind 15-MW reference turbines [2] supported by the VoltturnUS-S semisubmersible platform [3]. Following the design scope summarized in Table 1, the wind farm adopts a rectangular grid layout based on the site conditions of Sørlige Nordsjø II (SN2), Norway. The mooring systems are semi-taut and utilize suction anchors, while the dynamic power cables adopt lazy-wave configurations. The shallow-water reference design is developed in accordance with the requirements and methodology outlined in the *IEA Wind Task 49 Reference Floating Wind Array Design Basis* [1].

Table 1. Shallow-Water Design Specifications [1]

Scenario	Description
Key features	Mooring and dynamic cable designs that focus on addressing shallow water challenges
Design variants	Uniform seabed
Metocean	Sørlige Nordsjø II
Depth	60 m
Array layout	Rectangular grid-based layout
Platform type	VoltturnUS-S semi-submersible platform [3]
Mooring configuration	Chain-polyester semi-taut
Mooring layout	3-line mooring
Anchors	Suction anchor
Cable configuration	Lazy-wave

This report describes the methodology and technical details of the Task 49 shallow-water reference design. Section 2 outlines the site conditions, while Section 3 describes the semi-taut

chain–polyester–chain mooring system. Section 4 presents the suction anchor design, and Section 5 details the dynamic cable design. The wind farm layout, turbine positions, and cable routing are described in Section 6. Finally, Section 7 presents the cost modelling assumptions, methodology, and results.

2 Site Conditions

The Task 49 WP2 shallow-water floating array design is based on the reference site Sørlige Nordsjø II (SN2), located approximately 140 km off the Norwegian coast and covering an area of 2591 km² [4]. Figure 1 shows the location of SN2, which lies approximately 180 km from the nearest port. The site water depth ranges from 53 m to 70 m, making it suitable for both floating and bottom-fixed offshore wind turbines. On 29 March 2023, the Norwegian Ministry of Energy announced the competition for the first development phase of SN2, corresponding to a maximum installed capacity of 1500 MW. Meteorological and oceanographic (metocean) data for SN2 are available through the NORA3 database, which is generated using the non-hydrostatic regional numerical weather prediction model HARMONIE-AROME [5]. Based on the NORA3 dataset, Cheynet et al. [4] processed and fitted the environmental conditions into joint distributions of key wind and wave parameters. These site conditions are also included in the global reference site condition datasets developed under Task 49 [6]. The wind and wave roses for SN2 are presented in Figure 2.

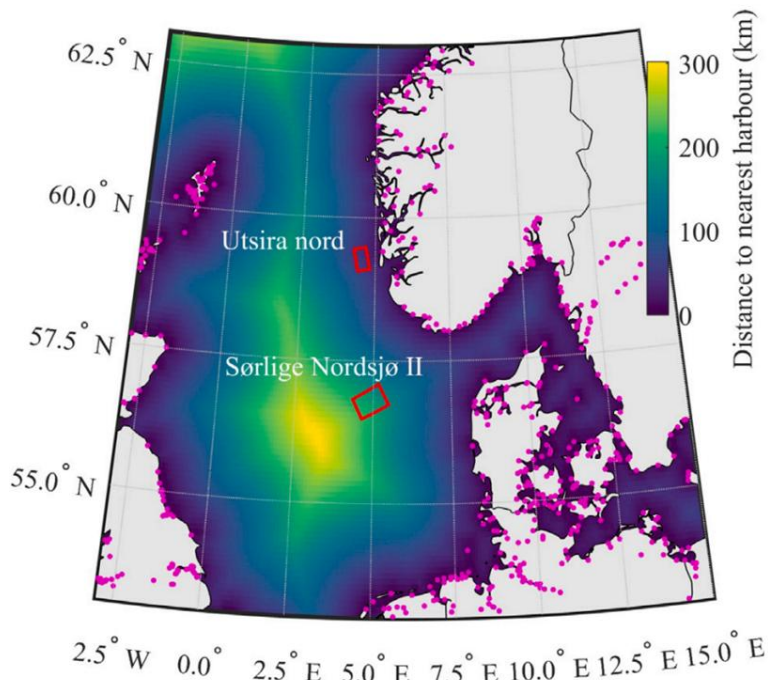


Figure 1. Location of SN2 [4].

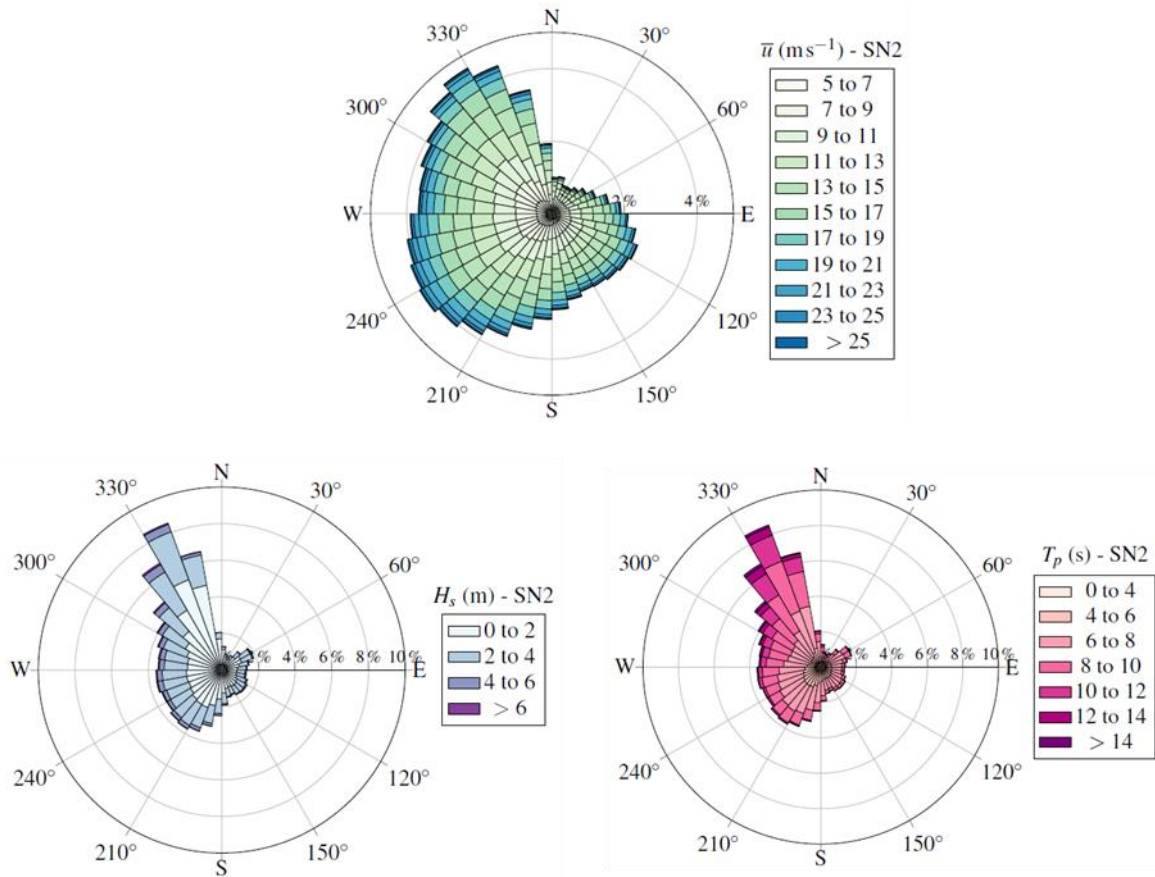


Figure 2. Polar histograms of the mean wind speed at 150 m height, significant wave height (Hs) and spectral peak period (Tp) at SN2 [4]

The processed metocean data are used to define the load cases for evaluating the performance of the mooring, anchor, and dynamic cable systems. The critical load cases were identified in [1] and include International Electrotechnical Commission (IEC) design load cases (DLCs) 1.6 and 6.1, which are used to assess structural performance under extreme environmental conditions. DLC 1.6 represents the operational condition of the wind turbine at rated wind speed, corresponding to the maximum aerodynamic thrust loading combined with severe wave conditions. DLC 6.1 represents a 50-year storm condition with the wind turbine in a parked state. For current loading, current profiles with 1-year and 5-year return periods are adopted for DLC 1.6 and DLC 6.1, respectively. The environmental conditions associated with the selected load cases are summarized in Table 2, while the corresponding current profiles are presented in Table 3.

Table 2. Metocean Parameters for Critical Strength Load Cases

Parameter	DLC 1.6	DLC 6.1
Wind speed (m/s)	10.59	39.44
Turbulence intensity	0.110	0.099
Shear	0.08	0.08
Wave height (m)	7.5	11.7
Wave period (s)	13.2	15.1
Current speed at surface (m/s)	0.82	0.98

Table 3. Current Profiles at Different Return Periods

Depth	1-year	5-year
Surface	0.82	0.98
3 m	0.76	0.92
10 m	0.69	0.85
15 m	0.66	0.81
25 m	0.58	0.72
50 m	0.45	0.58
55 m	0.42	0.54
57 m	0.40	0.52
59 m	0.35	0.46
60 m	0.00	0.00

In accordance with the design basis [1], the depth-dependent marine growth thickness on the mooring lines and cable is shown in Table 4. The thickness is added to arrive at the end-of-life (EOL) state of the submerged components. The density of the marine growth is 1300 kg/m^3 .

Table 4. Marine Growth Thickness at Two Depth Ranges

Depth Range	Marine Growth Thickness (mm)
Surface–40 m	100
Below 40 m	50

3 Mooring Design¹

The chain-polyester semi-taut mooring design is chosen due to its adaptability in shallow water depths, where conventional chain-only mooring systems are challenged by high tension spikes. With the polyester ropes' making up the majority of the length, its elastic restoring capability is favourable when the water depth is limited, and the weight of mooring line is low. The performance of synthetic fibre-based mooring lines has been proven to provide desirable characteristics in shallow waters [7].

3.1 Design Assumptions and Requirements

The design of mooring system is carried out based on the design requirement outlined in the design basis [1]. Widely adopted design guidelines such as the ABS [8] and DNV guidelines [9] are also referred to. The criteria used for the mooring design are summarized in Table 5.

Table 5. Mooring Design Criteria

Criteria	Requirement
Maximum tension	<p>The design tension safety factor (SF) requirement per ABS guidelines [8] for nonredundant stationkeeping systems must be greater than 2 for DLC 1.6 and DLC 6.1 where SF is defined as the ratio of minimum breaking load (MBL) of the mooring line to maximum tension value (T_{max}):</p> $SF = \frac{MBL}{T_{max}}$ <p>The design tension is defined as the the maximum tension observed from 10 3-hour realizations.</p>
Line slackness	The minimum tension in the line in all realizations must be greater than a nominal value of 100 kN for DLC 1.6 and DLC 6.1.
Rope zero ground contact	The polyester segments may not contact the seafloor (to avoid abrasion).
Maximum horizontal platform displacement	The maximum horizontal displacement of the platform must be less than 25% of the water depth (15 m).
Fatigue	The SF for the accumulated fatigue damage must be greater than 3, considering a 25-year lifetime.

¹ Parts of the technical contents in this section are included in “Lee, C. F., Mulas Hernando, D, Feng J., Ong, M. C., Techno-Economic Assessment of a 1-GW Floating Offshore Wind Farm at Intermediate Water Depths in the North Sea, *submitted for journal publication*”. The information about the article will be updated once the article is accepted for publication.

3.2 Design Approach

The design process started by basing on the properties of the VoltturnUS-S chain mooring system. The same chain diameter, anchor radial spacing and the fairlead pre-tension are adopted. An intermediate polyester rope segment is used to connect the top chain and ground chain segments. To avoid seabed contact of the polyester ropes, subsea buoys are placed at the start of the ground chain and at the midpoint of the polyester ropes. Placement of clump weights along the top chain segments is also carried out to prevent slack in the mooring lines.

While keeping the fairlead pre-tension constant, the length of each segment, number of clump weights and the positions of the subsea buoys are optimized iteratively under DLCs 1.6 and 6.1. At such water depth, mooring design is highly sensitive to the additional weight throughout its lifetime due to marine growth. This causes a drastic change in mooring configuration between the start-of-life (SOL) and end-of-life (EOL) states. In this work, the EOL configuration is assumed for both ultimate limit states (ULS) and fatigue limit states (FLS) evaluation, in which EOL marine growth and corrosion-adjusted MBL are taken into account.

The dynamic simulations were performed using SIMA v4.8.1 [10]. The following assumptions/simplifications were made in the dynamic simulations:

- For ULS evaluation, wind, wave, and current loads are considered, with current being modelled as inducing constant force. For FLS evaluation, only wind and wave loads are considered to limit the number of environmental parameters involved in fatigue bin generation. While current load contributes to the mean loads, its contribution can be simplified as having negligible effects on fatigue accumulation.
- For ULS evaluation, wind, wave, and current are assumed to be directionally aligned. As shown in Figure 3, two environmental headings are considered, i.e., 0° (loading with one Line 1 directly upwind) and 180° (loading with Line 1 directly downwind). For FLS evaluation, the wind and wave directions are according to the fatigue bins based on the metocean data at SN2.

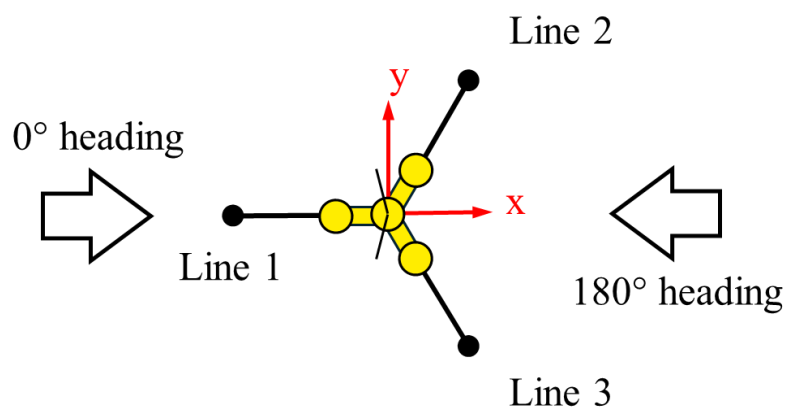


Figure 3. Environment headings used for strength load cases

3.3 Mooring Design Description

Figure 4 shows the semi-taut mooring design for the shallow water depth. Each mooring line consists of three segments; a top chain segment connected to the fairlead, an intermediate polyester rope segment and a ground chain segment connected to the anchor. Clump weights

are placed along the top chain segment to increase the line weight and to reduce the tension spikes. This, coupled with a long polyester rope segment is critical to the performance of mooring system in shallow water depths as shown in [11]. The mooring design parameters are given in Table 6.

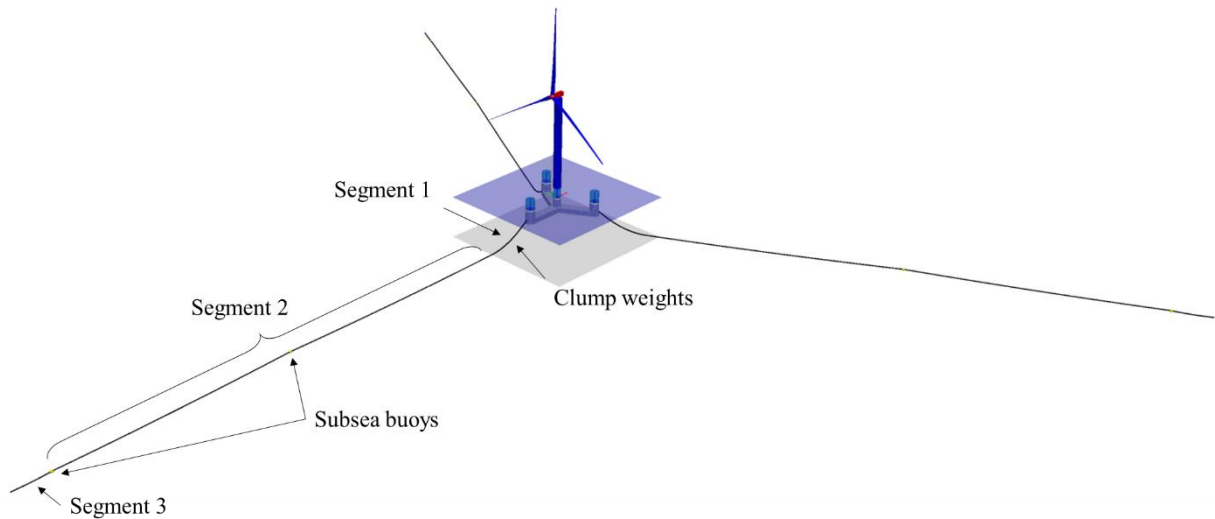


Figure 4. VoltturnUS-S platform and shallow-water mooring system

The chain properties are according to [1] while the polyester rope properties are provided in [12]. Since the EOL state is assumed, the equivalent line properties are derived considering marine growth and corrosion allowance. The EOL mooring line properties by segments are summarized in Table 7. For the polyester lines, the stiffness is modelled using Syrope [13], a visco-elastic approach that applies quasi-static stiffness to estimate the mean loads and offsets, while dynamic stiffness is used in dynamic simulations around the predicted mean offsets. Permanent elongation is considered by pre-stretching the rope to an anticipated highest mean tension over the entire service life.

Table 6. Mooring Design Parameters

Design Parameter	Value
Number of lines	3
Water depth	60 m
Anchor radius	837.6 m
Fairlead radius	58 m
Fairlead depth	14 m
Initial pretension	2,437 kN
Line section 1 type	185 mm studless R3 chain
Line section 1 length	75 m
Clump weight mass	10 ton
Clump weight number	11
Line section 2 type	277 mm polyester rope
Line section 2 length	651 m
Line section 3 type	185 mm studless R3 chain
Line section 3 length	50 m

Table 7. Mooring Line Properties Including Marine Growth

Segment	Type	MBL^a (kN)	Nominal Diameter (mm)	Marine Growth (mm)	Corrosion Allowance (mm/year)	Unstretched Length (m)	Volumetric Diameter (m)	Mass Density (kg/m)	Static Elastic Stiffness (N)
1	Chain	22,286	185	100	0.4	75	0.4696	845.79	2.61×10 ⁹
2	Polyester	22,563	277	50	-	651	0.2164	117.47	3.16×10 ⁸
3	Chain	22,286	142	50	0.4	50	0.3944	708.98	2.61×10 ⁹

^a The MBL value for chain presented in the table is the value without correction for corrosion allowance

3.4 Performance Results

The mooring system is evaluated against the ULS design criteria using ten random 3-hour realizations in SIMA for the considered load cases and headings. For FLS evaluation, one 3-hour realization is simulated for the environmental parameters in each fatigue bin.

3.4.1 Mooring Line Tension

The average mooring line tensions under all load cases are presented in Figure 5. Line 1 experiences the highest mean tension under DLC 1.6 at a 0° heading, corresponding to the rated wind speed operating condition. Figure 6 presents the maximum and minimum mooring line tensions, where the extrema for each line are obtained from the absolute maximum and minimum values across all realizations. The governing load case is DLC 6.1 at a 0° heading, for which both the maximum and minimum tensions occur in Line 1. The maximum tensions in all three lines remain below the specified MBL, while the minimum tensions remain well above the 100 kN threshold, indicating that no slack-line events occur (as required by the design criteria in Table 5).

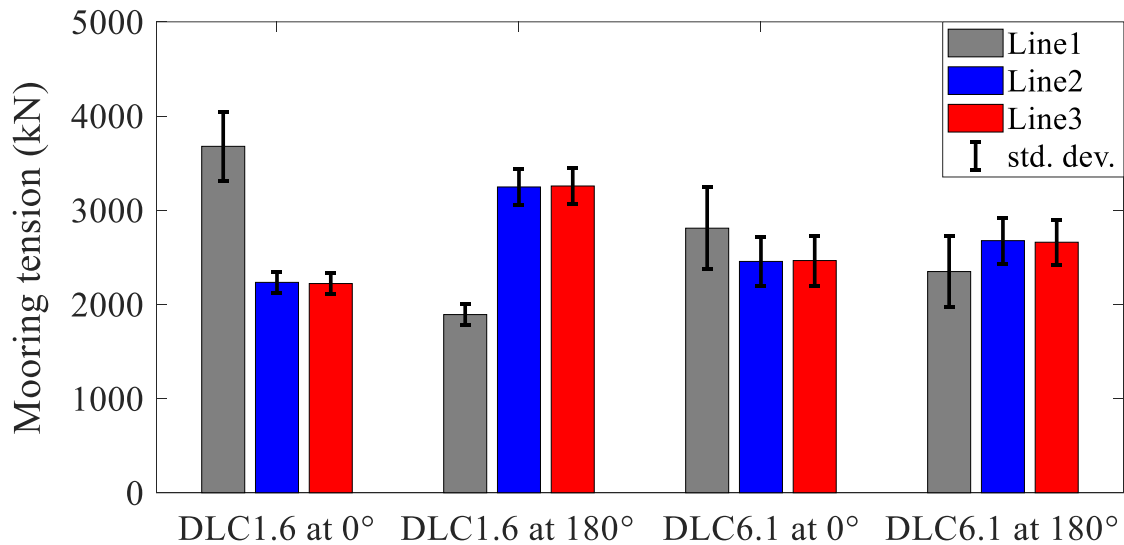


Figure 5. Line tension statistics

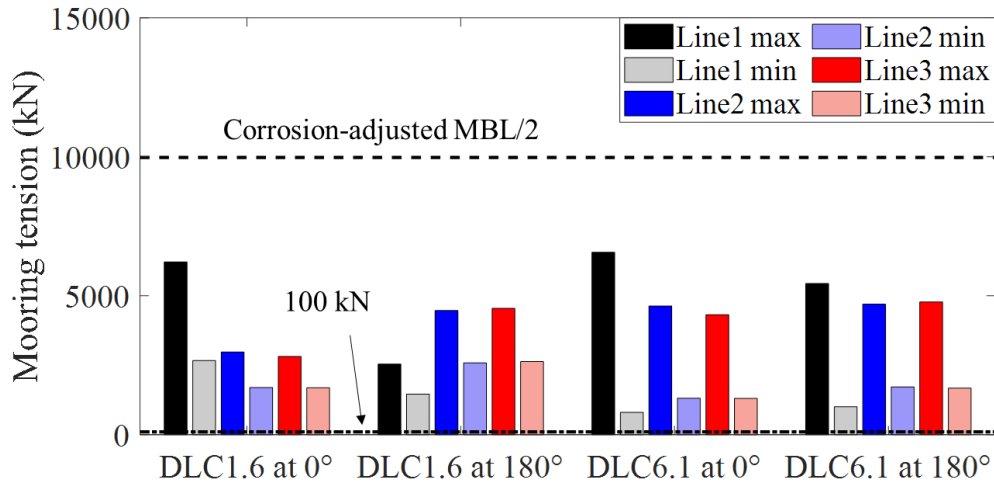


Figure 6. Line tension maximum and minimum values

3.4.2 Rope Ground Contact

To check for any contact between the polyester rope and the seabed, the vertical elevation envelopes for Line 1 are plotted for the limiting case of DLC 6.1 at 0° and 180° headings as shown in Figure 7 and Figure 8, respectively. Line 1 is selected as it is where minimum tension occurs. Figure 7 and Figure 8 show that the lowest elevation of the polyester ropes is at the end of the polyester rope, which sits approximately 1.5 m above the seabed. However, due to it being at the end of line and the fact that a subsea buoy is connected at that point, its downward movement is limited.

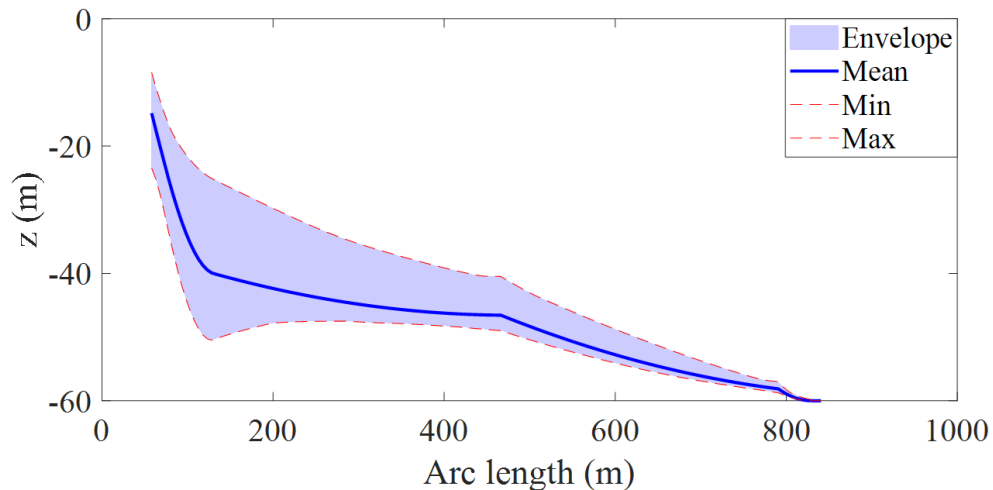


Figure 7. Line 1 Vertical Elevation Envelope under DLC 6.1 at 0°.

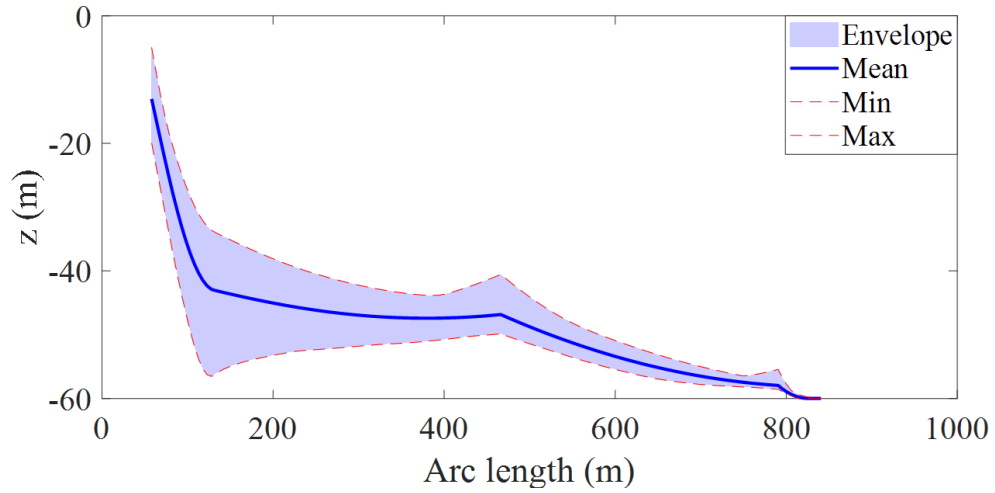


Figure 8. Line 1 Vertical Elevation Envelope under DLC 6.1 at 180°.

3.4.3 Maximum Horizontal Platform Displacement

The statistics of maximum horizontal platform displacement across all realizations are presented in Figure 9. For each load case, the environmental heading of 180° represents the limiting case with the worst-case maximum displacement of approximately 14.88 m in the DLCs, which is less than 25% of the water depth (15 m).

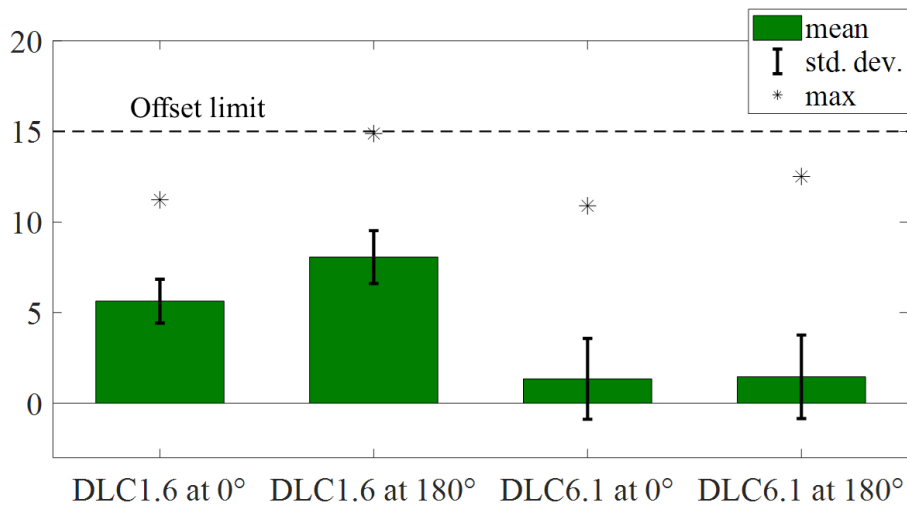


Figure 9. Statistics of the platform horizontal displacement

3.4.4 Fatigue Analysis

The mooring component's lifetime fatigue damage is calculated based on a set of environmental conditions representing the long-term metocean condition of the SN2 site [6]. The metocean conditions are described using five environmental variables, i.e., \bar{u} , H_s , T_p and the incoming directions of wind, θ_{wind} , and waves, θ_{waves} . A total of 100 fatigue bins are generated using the Maximum Dissimilarity Algorithm (MDA) based on hindcast data provided in NORA3. As the mooring chain is the critical component, this work will limit the effort in evaluating the fatigue damage of the chain.

The calculation of fatigue damage is through Miner's rule [14], in which the characteristic damage in a mooring chain is accumulated over cyclic loading and summed up for all bins. The mooring chain's capacity against tension fatigue can be obtained from S-N curves for studless chain (intercept parameter of 6.0×10^{10} and slope parameter of 3.0) [15]. The rainflow counting method is used to calculate the number of load cycle corresponding to each stress range in the realization. The total long-term fatigue damage is obtained by extrapolating the fatigue damage at each bin and summing them over a 25-year service lifetime. As the wind is predominantly coming from the 330° to 210° , and waves are concentrated around 330° , the mooring orientation that maximizes the fatigue damage is chosen as the limiting case. Figure 10 shows the mooring line orientation that the fatigue analysis is carried out on.

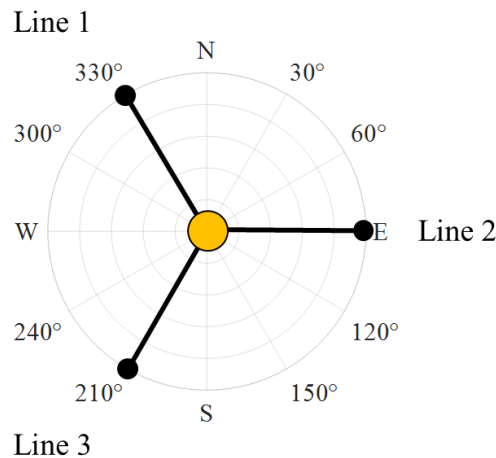


Figure 10. Mooring line orientation for fatigue analysis.

The resulting fatigue damage accumulated over 25 years for the three mooring lines are presented in **Figure 11**. Line 1 and Line 3 are the ones that sustain the largest fatigue damage as they are more directionally aligned to the environmental loadings. The FLS analysis shows that the fatigue damage on all mooring lines meet the requirement with safety factors greater than 3.

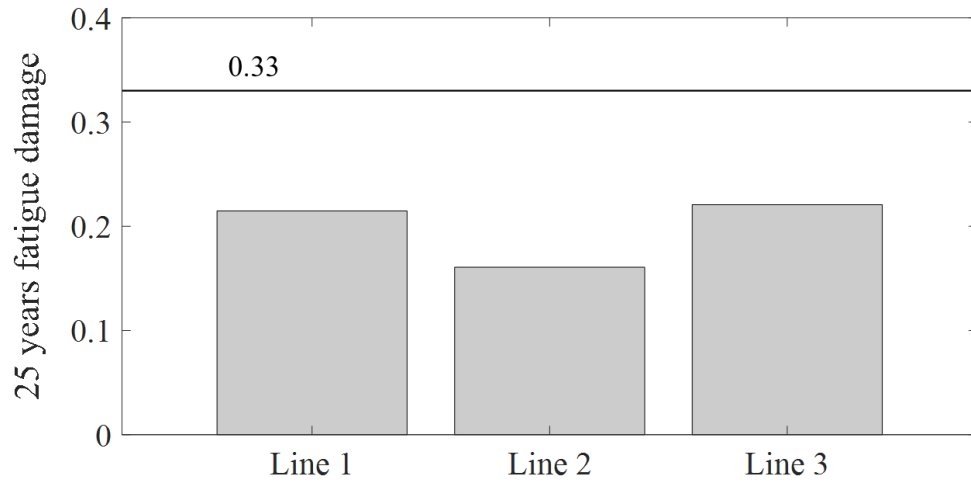


Figure 11. Accumulate fatigue damage of the mooring lines over 25 years.

4 Anchor Design

For mooring systems in shallow water depths, the lack of suspended mooring line weight results in little contribution of vertical restoring force. Hence the majority of the vertical restoring force will have to come from the anchors. Hence, suction anchors, best known for their capability in sustaining vertical anchor loads are selected for the shallow-water reference design. Suction anchors are also selected due to their characteristics to be less dependent on the seabed condition and reduced seabed disturbance.

4.1 Design Assumptions and Requirements

The suction is designed with the assumption of normally consolidated clayed seabed with undrained shear strength that varies with depth, i.e., $s_u = s_{um} + kz$, where s_{um} is the shear strength at mudline, k is the strength increase gradient and z is the depth below the mudline.

Anchor load demand for the mooring system is obtained through simulations for ULS evaluation with DLC 6.1 as the governing case. The anchor load at seabed is converted to the padeye, located at 2/3 of the anchor skirt length measured from the top through the inversed catenary. The padeye loadings in the vertical and horizontal directions are checked against the anchor capacity. Anchor capacity is derived based on plastic limit analysis (PLA) following [16]. For this case, safety factors of 2.4 for vertical loading and 1.92 for horizontal/inclined loading were applied in accordance with API RP 2SK [17] and ABS guidelines [8].

4.2 Anchor Design Description

The suction anchor in this report is sized manually and the anchor demand checked against the capacity. The design is deemed acceptable when the vertical and horizontal loads at padeye satisfy the safety factor requirement. The capacity curve generated for the selected suction anchor is shown in Figure 12 while Table 8 summarizes the key design parameters and the final dimensions of the suction anchors.

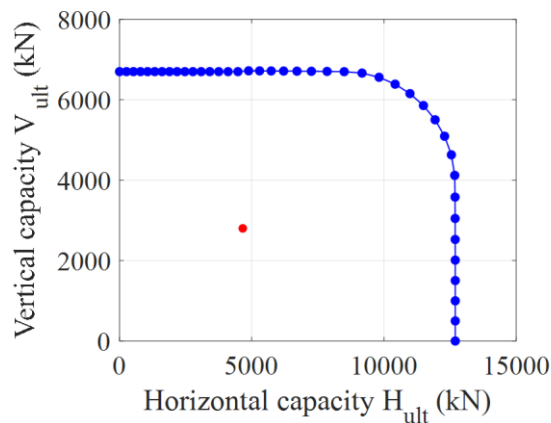


Figure 12. Suction anchor capacity.

Table 8. Final Suction Anchor Configuration and Verification Summary

Parameter	Symbol and Units	Value
Governing design case	-	DLC 6.1
Water depth	-	60 m
Soil profile	-	Clay ($s_u = 5 + 1.5z$ kPa)
Anchor type	-	Suction caisson
Diameter	D (m)	5.0
Length	L (m)	15.0
Padeye depth	-	10 m from the top
Vertical load demand	V_{max} (MN)	2.55
Capacity safety factor	-	2.63 (>2.4)
Horizontal load demand	H_{max} (MN)	4.80
Capacity safety factor	-	2.64 (>1.92)
Steel mass	W (t)	133

5 Dynamic Cable Design²

Dynamic cables rated at 66 kV are adopted throughout the wind farm, with different conductor sizes depending on the FOWT’s position in the serial connection relative to the offshore substation (OSS). Based on the wind farm configuration, turbine layout and cable routing, three conductor sizes (300, 630, and 1,000 mm²) are identified. The detailed performance analysis of the dynamic cable in this study is carried out based on the conductor size of 630 mm². The dynamic cable adopts a lazy-wave configuration.

5.1 Design Assumptions and Requirements

The design assumptions and requirements for the dynamic cables follows [1] and the properties of the dynamic cable are adopted from [18]. The properties of the cable for all conductor sizes are summarized in

Table 9. Cable Type 2 will be modelled and analyzed. For the in-line buoyancy modules, synthetic foam-based packing with a density of 500 kg/m³ is assumed. The general properties for each module are listed in

Table 10. A bend stiffener is used to limit the bending curvature at the hang-off point (HOP). The geometric properties of the bend stiffener are shown in Figure 13.

Table 9. Dynamic Cable Properties

Parameter	Cable Type 1	Cable Type 2	Cable Type 3
Conductor size (mm ²)	300	630	1,000
Outer diameter (m)	0.161	0.184	0.203
Linear mass density (kg/m)	36.66	55.76	75.74
Axial stiffness (N)	469 x 10 ⁶	658 x 10 ⁶	854 x 10 ⁶
Bending stiffness (N·m ²)	Curvature-dependent		

² Parts of the technical contents in this section are included in “Lee, C. F., Mulas Hernando, D, Feng J., Ong, M. C., Techno-Economic Assessment of a 1-GW Floating Offshore Wind Farm at Intermediate Water Depths in the North Sea, *submitted for journal publication*”. The information about the article will be updated once the article is accepted for publication.

Minimum breaking load (MBL) (kN)	383.2	500	698.4
Minimum bending radius (MBR) (m)	2.41	2.5	3.05

Table 10. Buoyancy Module Properties

Parameter	Value
Outer diameter (m)	0.63
Inner diameter (m)	0.184
Length (m)	1.0
Displacement (m ³)	0.285
Density (kg/m ³)	500

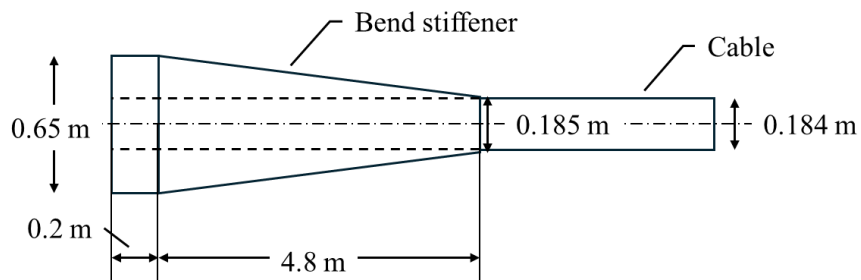


Figure 13. Bend Stiffener Dimensions

Two critical design parameters for a dynamic cable are the maximum allowable tension and bending curvature. With the two parameters being dependent of each other, the utilization factor, as proposed in [18], is used as the ULS design criteria in this work. The tension-curvature relationship is presented in Figure 14. Under all simulated environmental conditions (DLCs 1.6 and 6.1), the instantaneous curvature and tension along the cable are to fall under the capacity curve with an 80% utilization limit.

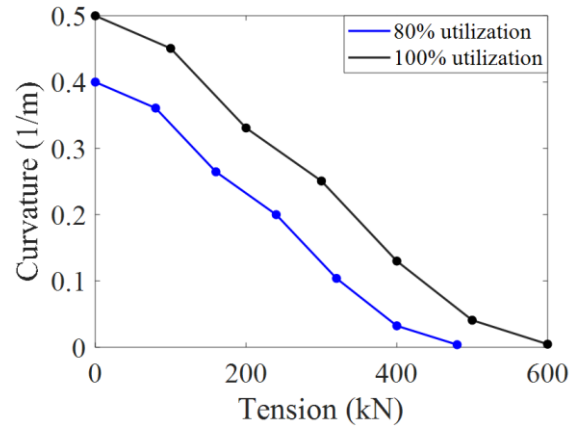


Figure 14. Cable Capacity Curves [18]

5.2 Design Approach

Parametric optimization is carried out to determine the geometric parameters (l_1 , l_2 and l_3) of the dynamic cable. Hydrostatic equilibrium of the dynamic cable is evaluated to locate the combination of geometric parameters that minimizes the curvature and tension at three different offset locations: the neutral position (0 m), the extended position away from the touchdown point (TDP) (+15 m) and the offset towards the cable TDP (-15 m). The numerical boundary of the optimization scheme is shown in Figure 15. At each iteration, the algorithm checks for the validity of the numerical boundary, that is, no change in the cable tension is observed when the numerical boundary and the touchdown length (l_{TD}) are extended. This ensures that a constraint on the touchdown length is imposed. Moreover, the overbend of the cable (buoyancy segment) is limited to 40 m below the mean water surface to avoid the region where marine growth is the most extensive.

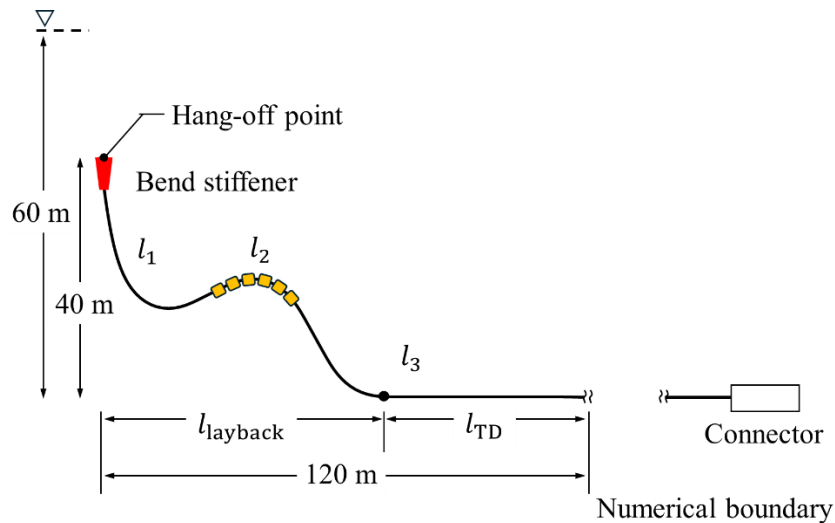


Figure 15. Numerical Boundary of the Parametric Optimization.

Once the geometric parameters are obtained, the dynamic cable is modelled and simulated using SIMA in a fully coupled manner. A fully coupled model that incorporates platform, mooring and cable dynamics allows for the collection of results under the same set of simulations. Since 0° and 180° are evaluated for both DLCs, the dynamic cable is oriented either along or against the environmental loads. The different cross sections of the dynamic cable, including bare cable, cable segment with marine growth, cable segment with buoyancy modules and marine growth and cable with bend stiffener are modelled with equivalent cross section properties. The considered environmental heading directions for the lazy-wave and suspended cable designs are shown in Figure 16.

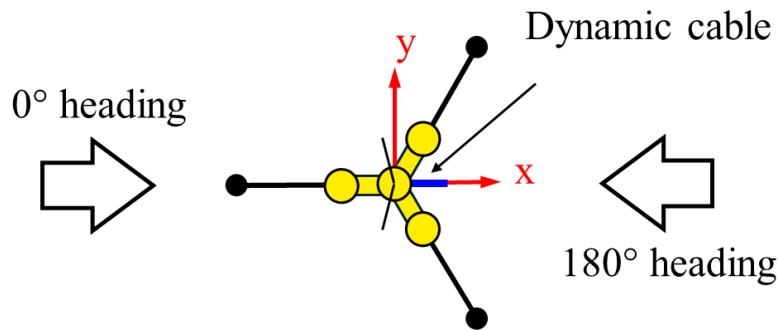


Figure 16. Dynamic Cable Orientation.

5.3 Dynamic Cable Design Descriptions

Based on the initial lazy-wave configuration from the parametric optimization, full details of the dynamic cable components use for the numerical model are provided in

Table 11. The total cable length is 156 m, with a 45 m buoyancy segment length. Based on the specifications provided in

Table 10, 23 buoyancy modules are required with a 1 m gap between the ends of adjacent modules.

Table 11. Lazy-Wave Cable Design Parameters

Properties	Value
Conductor Size (mm ²)	630
Span (m)	120

Total cable length (m)	156
Bend stiffener length (m)	5
l_1 length including bend stiffener (m)	54
l_2 length (m)	45
l_3 length (m)	57
Number of buoyancy modules	23
Buoyancy module spacing (m)	1
Averaged diameter of buoyancy section (m)	0.39
Averaged mass of buoyancy section (kg/m)	83.38

Marine growth on the dynamic cable at EOL is considered based on the assumptions in Table 4. 15 m of cable after the exit of bend stiffener is modelled with 100 mm of marine growth while the rest of the segments are modelled with 50 mm. The equivalent cable properties considering marine growth are provided in Table 12. With a 60 m water depth and a draft of 20 m, the distance between the cable HOP and the seabed is 40 m. The limited water column presents a significant challenge for the dimensioning of the dynamic cable as its configuration is highly sensitive to current loads and the change in submerged weight due to marine growth. To ensure that the dynamic cable configuration is acceptable in SOL and EOL, minor adjustment is made to the parameters from the optimization algorithm. To show the sensitivity of the dynamic cable to current loads and marine growth, the hydrostatic lazy-wave cable profiles are shown in Figure 17.

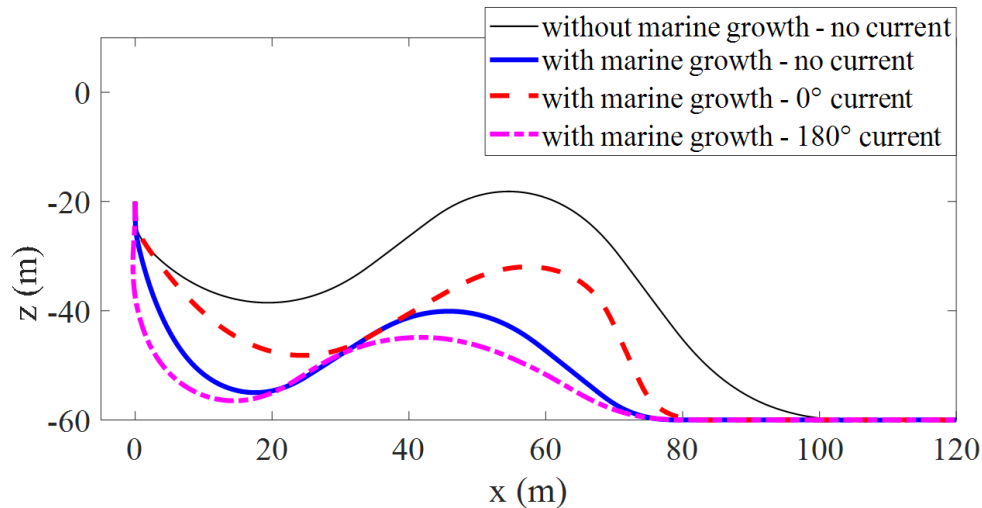


Figure 17. Hydrostatic Lazy-wave Cable Profiles.

Table 12. Cable Equivalent Properties With Marine Growth

Properties	Value
Length of cable with 100 mm of marine growth	15
Averaged diameter of cable with 100 mm of marine growth (m)	0.59
Averaged mass of cable with 100 mm of marine growth (kg/m)	285.88
Length of cable with 50 mm of marine growth (m)	136
Averaged diameter of cable with 50 mm of marine growth (m)	0.49
Averaged mass of cable with 50 mm of marine growth (kg/m)	132.73

5.4 Performance Results

The ULS evaluation of the dynamic cable is carried out under DLC 1.6 and 6.1 and the tension and curvature combinations under all realizations are checked against the capacity curve of 80% utilization. Two locations along the dynamic cable are identified as the critical points, i.e., regions close to the HOP and TDP.

5.4.1 Cable Tensions

The cable tension statistics in DLCs 1.6 and 6.1 are shown in Figure 18. The simulated tensions and curvatures fall below the capacity curve of 80% utilization. The mean tension at HOP is the highest for all DLCs. Despite having a lower mean tension at TDP, the standard deviations are significantly higher as compared to that at HOP. This is likely because the cable orientation at TDP is more directionally aligned to the direction of the environmental loadings, while the cable is oriented vertically at HOP. Subjected to 0° loadings, the computed negative mean axial force at the TDP is interpreted as due to the modelled constant axial stiffness in the low-tension touchdown zone. This simplification is used to ensure modelling efficiency, with curvature being the more critical parameter under low-tension conditions.

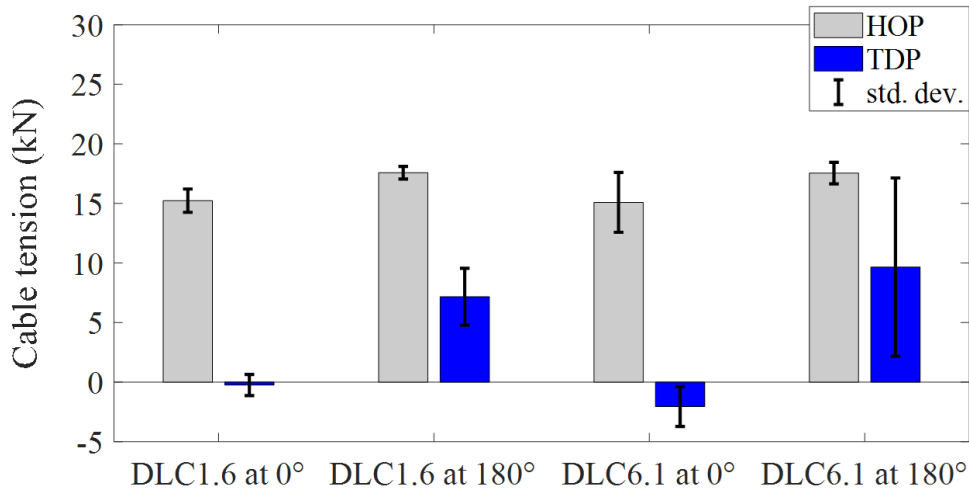


Figure 18. Dynamic cable tension statistics at HOP and TDP.

Figure 19 shows the maximum cable tensions for both 0° and 180° environmental headings from all realizations. The maximum tension occurs at TDP, when the system is subjected to 180° loadings that displaces the platform away from the TDP. At HOP, the maximum tension is less affected by the loading direction due to the cable orientation. The configuration of the dynamic cable under loadings from different directions and its effect on the tension at different positions is best visualized in Figure 17.

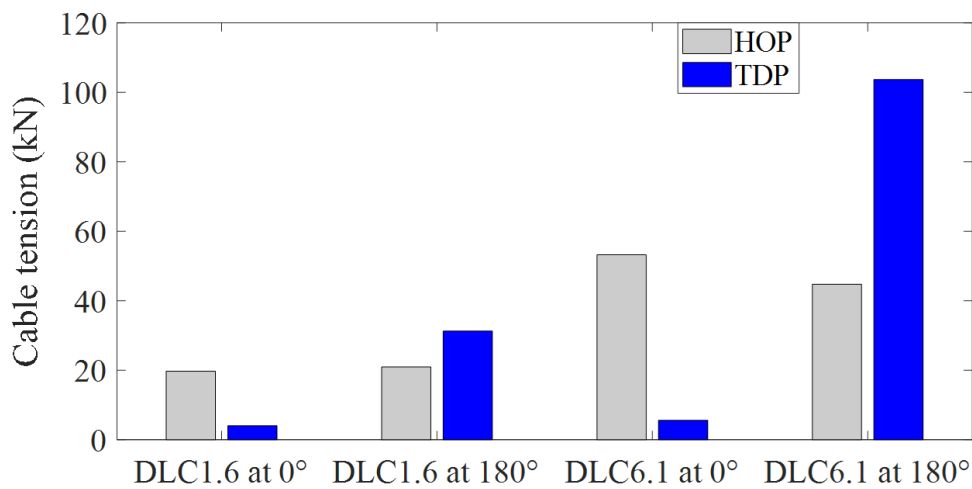


Figure 19. Dynamic cable maximum tensions at HOP and TDP.

5.4.2 Cable Curvatures

The cable curvatures measured at HOP and TDP are shown in Figure 20. The curvatures at both locations are higher when subjected to 0° loadings due mainly to the effect of current on bending close to both regions. The maximum curvature for the suspended cable designs is shown in Figure 21. In terms of bending curvature, the TDP region emerges as the critical region as the curvature at HOP is constrained by the bend stiffener.

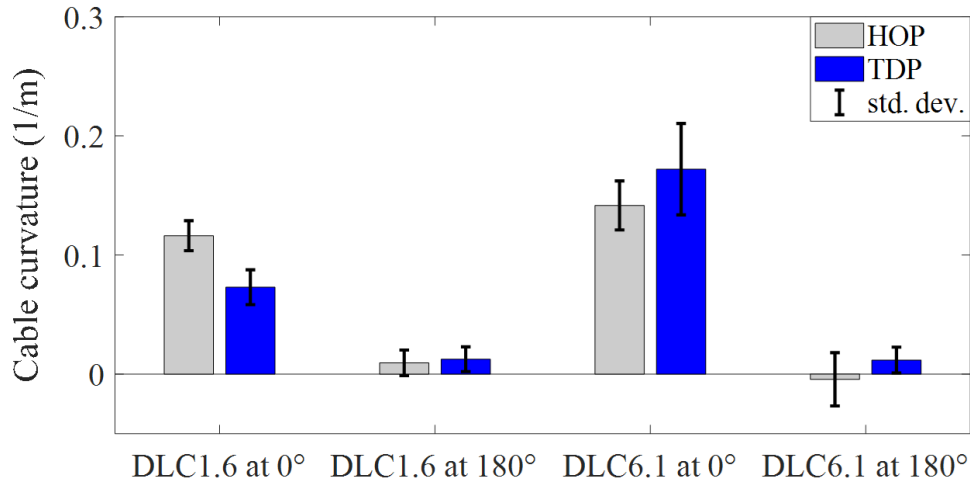


Figure 20. Dynamic cable curvature statistics at HOP and TDP.

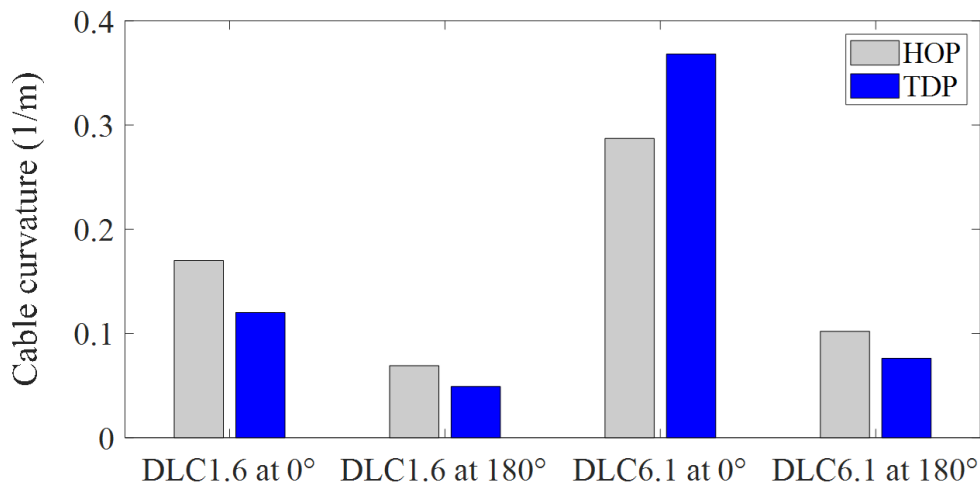


Figure 21. Dynamic cable maximum curvatures at HOP and TDP.

5.4.3 Cable Ground Contact

The vertical displacement envelope along the length of the cable under DLC 6.1 at 0° and 180° are shown in Figure 22 and Figure 23, respectively. With the environmental heading of 180° , current pushes the lazy wave away from the TDP which leads to the lowest point of the sagbend being in contact with the seabed. This is raised as a point of concern during the cable design. Future studies on dynamic cables in shallow waters should consider different cable configurations or suggest potential solutions if seabed contact inevitable.

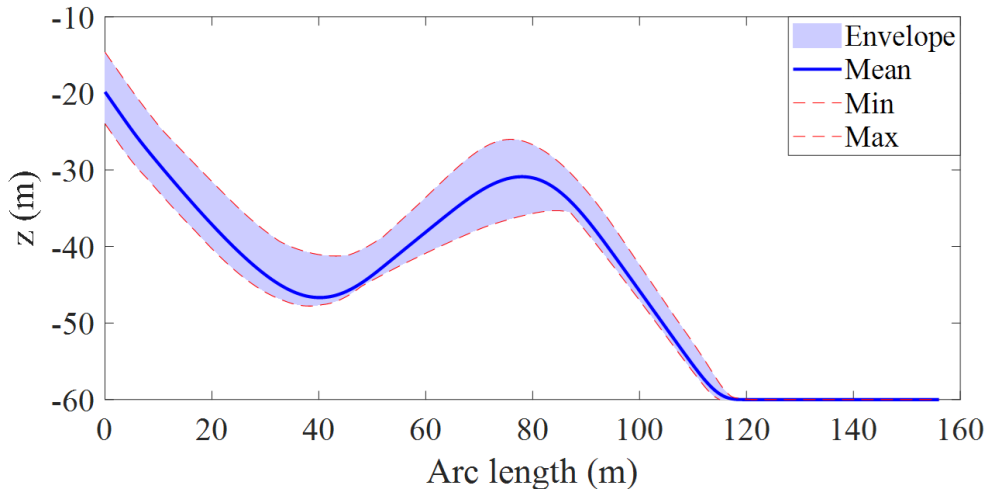


Figure 22. Cable Vertical Displacement Envelope under DLC 6.1 at 0° .

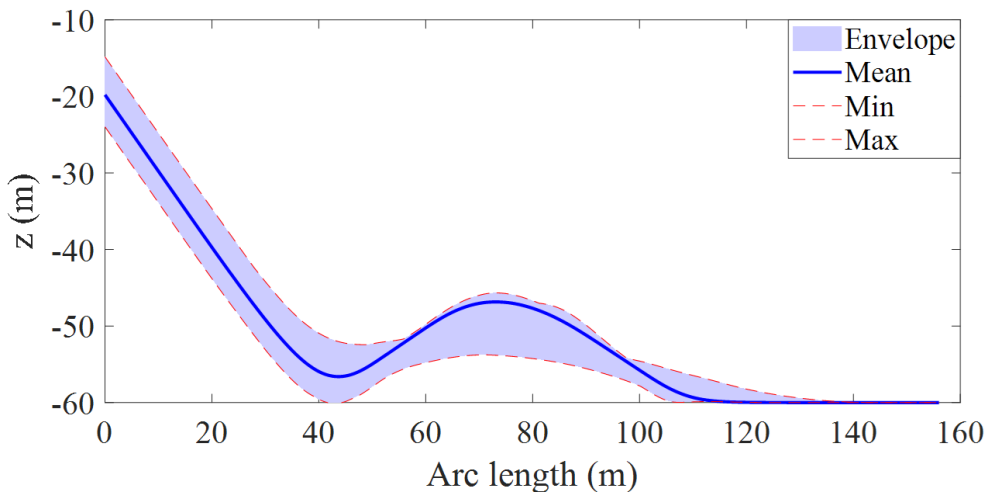


Figure 23. Cable Vertical Displacement Envelope under DLC 6.1 at 180° .

6 Layout³

The shallow-water reference wind farm adopts a regular grid-type configuration with a grid orientation of 60° , consistent with the orientation of the project area [19]. The grid orientation is illustrated in Figure 24. To provide a generic reference design for future studies, the layout is developed without considering seabed bathymetry. The spacing between adjacent rows and columns is fixed at 2 km, resulting in a rectangular boundary covering an area of 345 km². This area is determined based on an assumed power density of 2.88 MW/km², corresponding to the maximum permitted capacity of 1500 MW over a project area of 520 km² as specified by the ministry [19]. Given a rotor diameter (D) of 240 m for the reference turbine, the minimum spacing between adjacent turbines corresponds to approximately $8.33D$. This spacing is considered sufficient to prevent clashing between mooring lines. Although the configuration is not optimized for AEP, wake interference is expected to be minimal due to the relatively large turbine spacing.

The inter-array power cable system consists of 1 OSS connected to 8 branches of FOWTs, with each branch containing 8 or 9 FOWTs connected in series. Each dynamic cable that connects to a FOWT adopts a lazy-wave configuration, as described in Section 5. Each dynamic cable is subsequently connected to a static seabed cable routed towards the adjacent FOWT. Cable routing is performed manually with the objective of avoiding clashes with mooring lines and anchors along the cable path. The cable cross-sectional area (300, 630, or 1000 mm²) is selected based on the cumulative upstream power capacity transmitted towards the OSS.

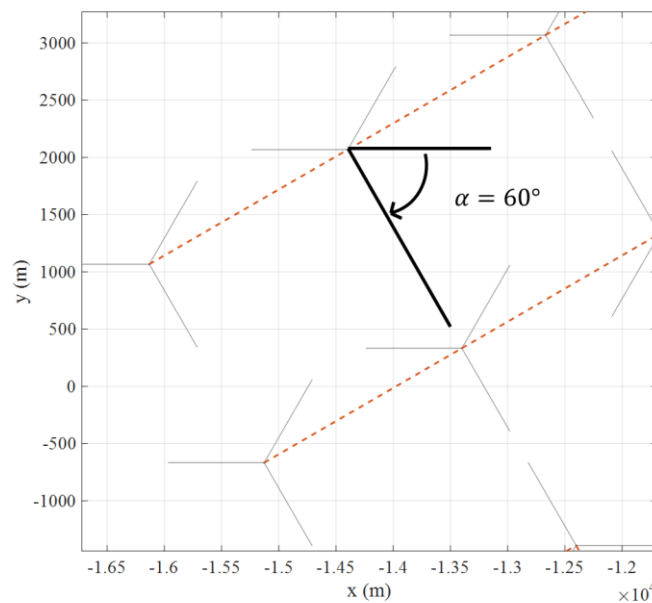


Figure 24. Orientation of the layout grid.

³ Parts of the technical contents in this section are included in “Lee, C. F., Mulas Hernando, D, Feng J., Ong, M. C., Techno-Economic Assessment of a 1-GW Floating Offshore Wind Farm at Intermediate Water Depths in the North Sea, *submitted for journal publication*”. The information about the article will be updated once the article is accepted for publication.

The array layout, cable routing, and mooring orientations are shown in Figure 25. The parameters of the final array layout and mooring line orientation are summarized in Table 13. The reference point of the array layout is chosen to be the OSS, which is manually selected as the point closest to the assumed point of interconnection (POI) at Kvinesdal, Norway. Full coordinates of the turbine and OSS are provided in Table 14.

Table 13. Array Layout and Mooring Line Orientation Parameters

Parameter	Value
Turbine spacing Dx' (m)	2000
Turbine spacing Dy' (m)	2000
Grid rotation α ($^\circ$)	60
Mooring Line 1 heading ($^\circ$)	330

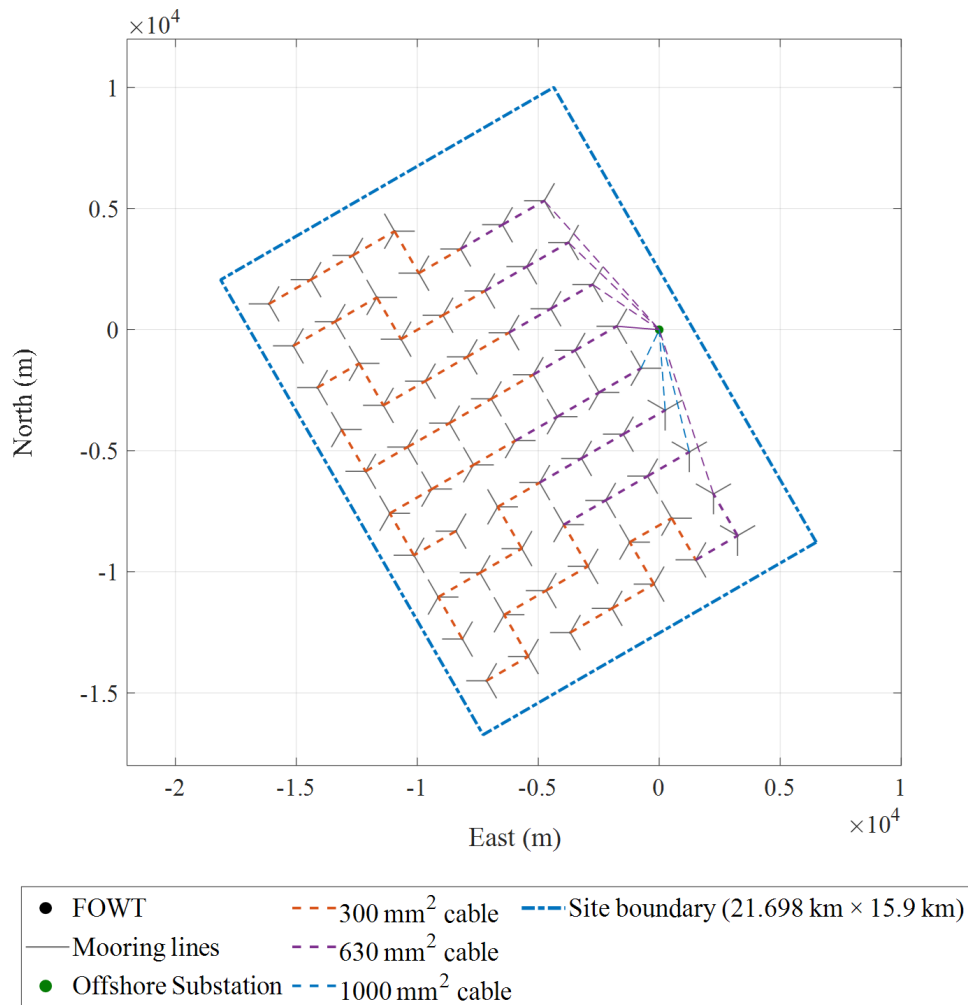


Figure 25. Array layout and cable routing

Table 14. Turbine and Substation Coordinates

Substation/ Turbine No.	Platform x (m)	Platform y (m)	Substation/ Turbine No.	Platform x (m)	Platform y (m)
OSS	0	0	Turbine 34	-7951.93	-1125.03
Turbine 1	-16148.10	1067.43	Turbine 35	-6951.92	-2854.16
Turbine 2	-15148.10	-661.71	Turbine 36	-5951.92	-4583.29
Turbine 3	-14148.10	-2390.84	Turbine 37	-4951.91	-6312.43
Turbine 4	-13148.10	-4119.97	Turbine 38	-3951.91	-8041.56
Turbine 5	-12148.10	-5849.11	Turbine 39	-2951.90	-9770.69
Turbine 6	-11148.10	-7578.24	Turbine 40	-1951.90	-11499.80
Turbine 7	-10148.10	-9307.37	Turbine 41	-8219.88	3331.56
Turbine 8	-9148.08	-11036.50	Turbine 42	-7219.87	1602.42
Turbine 9	-8148.08	-12765.60	Turbine 43	-6219.87	-126.71
Turbine 10	-7148.08	-14494.80	Turbine 44	-5219.86	-1855.84
Turbine 11	-14416.10	2065.74	Turbine 45	-4219.86	-3584.98
Turbine 12	-13416.10	336.61	Turbine 46	-3219.85	-5314.11
Turbine 13	-12416.00	-1392.52	Turbine 47	-2219.85	-7043.24
Turbine 14	-11416.00	-3121.66	Turbine 48	-1219.84	-8772.38
Turbine 15	-10416.00	-4850.79	Turbine 49	-219.84	-10501.50
Turbine 16	-9416.03	-6579.93	Turbine 50	-6487.82	4329.87
Turbine 17	-8416.03	-8309.06	Turbine 51	-5487.81	2600.74
Turbine 18	-7416.03	-10038.20	Turbine 52	-4487.81	871.61
Turbine 19	-6416.02	-11767.30	Turbine 53	-3487.80	-857.53
Turbine 20	-5416.02	-13496.50	Turbine 54	-2487.80	-2586.66
Turbine 21	-12684.00	3064.06	Turbine 55	-1487.80	-4315.80
Turbine 22	-11684.00	1334.93	Turbine 56	-487.79	-6044.93
Turbine 23	-10684.00	-394.21	Turbine 57	512.22	-7774.06
Turbine 24	-9683.98	-2123.34	Turbine 58	1512.22	-9503.20
Turbine 25	-8683.98	-3852.48	Turbine 59	-4755.76	5328.19
Turbine 26	-7683.98	-5581.61	Turbine 60	-3755.75	3599.06
Turbine 27	-6683.97	-7310.74	Turbine 61	-2755.75	1869.92
Turbine 28	-5683.97	-9039.88	Turbine 62	-1755.75	140.79
Turbine 29	-4683.96	-10769.00	Turbine 63	-755.74	-1588.35
Turbine 30	-3683.96	-12498.10	Turbine 64	244.26	-3317.48
Turbine 31	-10951.90	4062.38	Turbine 65	1244.27	-5046.61
Turbine 32	-9951.94	2333.24	Turbine 66	2244.27	-6775.75
Turbine 33	-8951.93	604.11	Turbine 67	3244.28	-8504.88

7 Cost and Logistics Modelling⁴

This section describes the methodology and assumptions used to evaluate the costs, logistics, and energy production of the reference wind farm design. Simulation models for installation, operation and maintenance (O&M) and annual energy production (AEP) are used to estimate CapEx, OpEx, net AEP, and the levelized cost of energy (LCOE) [1].

7.1 Methodology

The LCOE is calculated using CapEx, OpEx, net AEP, and the fixed charge rate (FCR) [20], i.e., $LCOE = \frac{FCR \times CapEx + OpEx}{net\ AEP}$. CapEx includes the initial development and installation costs up to the point of interconnection while OpEx covers the O&M costs. The detailed cost categories are outlined in the National Laboratory of the Rockies (NLR) Cost of Wind Energy Review [21]. The calculation of net AEP accounts for wake, electrical, technical, environmental, and availability losses. These values are estimated using the modelling tools described below.

Four open-source tools from NLR are used in this analysis:

- Offshore Renewables Balance-of-System and Installation Tool (ORBIT): estimates balance-of-system (BOS) costs, installation costs, and logistics.
- Windfarm Operations and Maintenance cost-Benefit Analysis Tool (WOMBAT): estimates O&M costs, availability, and logistics.
- FLOW Redirection and Induction in Steady State (FLORIS): estimates AEP and wake losses
- Wind Asset Value Estimation System (WAVES): combines the outputs from ORBIT, WOMBAT, and FLORIS to calculate the LCOE.

ORBIT uses a discrete-event simulation approach to model offshore installation activities and weather-related delays [22]. WOMBAT simulates maintenance activities, component failures, and repair logistics to estimate OpEx and wind farm availability [23]. FLORIS is a steady-state wake model used to evaluate wind farm performance and wake losses under different site conditions and layouts [24]. WAVES integrates the outputs from these tools together with financial assumptions and additional loss factors to estimate the overall LCOE [25].

7.2 Inputs and Assumptions

This subsection summarizes the key assumptions used in the analysis. These simulations were conducted using ORBIT version 1.2.4, WOMBAT version 0.12.2, FLORIS version 4.5.1, and WAVES version 0.6.1.

⁴ Parts of the technical contents in this section are included in “Lee, C. F., Mulas Hernando, D, Feng J., Ong, M. C., Techno-Economic Assessment of a 1-GW Floating Offshore Wind Farm at Intermediate Water Depths in the North Sea, *submitted for journal publication*”. The information about the article will be updated once the article is accepted for publication.

7.2.1 Plant Characteristics Summary

For this design variant, the cost and logistics models explicitly simulate installation activities and associated costs under site-specific conditions representative of the SN2 site. Costs and masses for the mooring system (taut lines with suction pile anchors) and intra-array cable system are precalculated based on the design characteristics described earlier in this report and incorporated directly as procurement cost inputs. Additional details on these component costs and masses are provided in Section 0.

To model the export system costs and the installation and O&M logistics of this reference plant, assumptions were made regarding the distances between the offshore substation and the POI, as well as between the wind farm and the installation and O&M port. For this analysis the Kvinesdal connection point was selected as the POI. The POI is one of the options considered for the current planned bottom-fixed wind farm under development. For the simulation of operation and construction activities, the Mandal Windport is designated as both the construction and O&M port due to its proximity to the selected site. Figure 26 shows the distance of the reference site with respect to the POI and the construction and O&M port, with the coordinate of the OSS used as the reference point.

The metocean data of the SN2 is used as input for installation and O&M simulations. Installation was assumed to begin in 1998, and operations (generation and O&M) were modelled with data from 1989 through 2008, providing 20 years of operational data for the analysis.

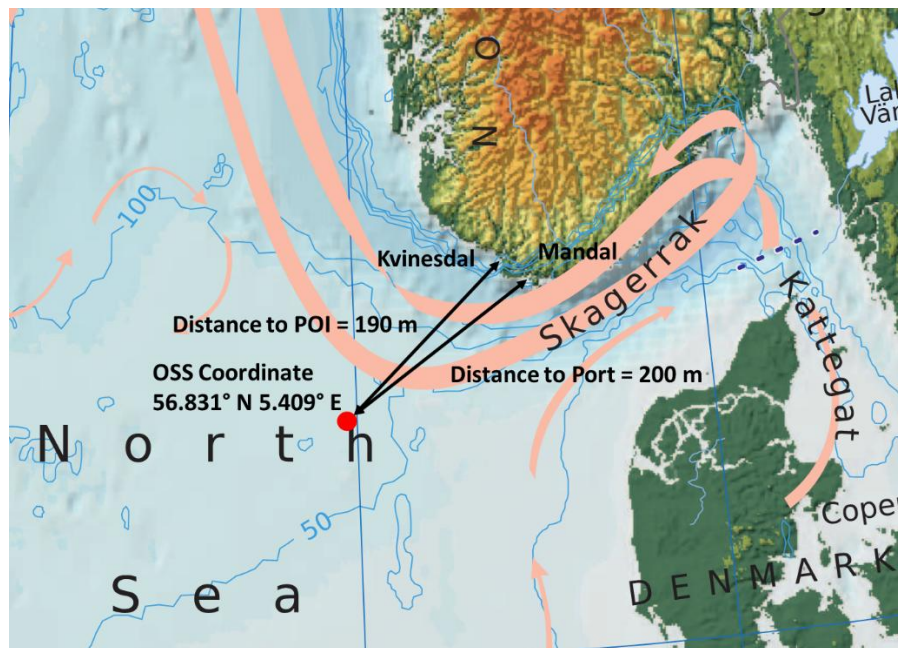


Figure 26. SN2 site location. Distances from OSS to assumed POI and construction port shown are used for cost and logistic modelling.

7.2.2 Task 49 Design Basis Cost and Logistics Considerations

Several recommendations and considerations from the Task 49 design basis cost and logistics guidance [1] were incorporated into this analysis. Table 15 summarizes the key considerations by LCOE driver.

Table 15. Summary of Design Basis Considerations by Key LCOE Driver

LCOE Driver	Assumptions
FCR	<ul style="list-style-type: none"> Pre-tax FCR was calculated without adjustments for depreciation, based on assumptions from [1], including an inflation rate of 2.5%, cost of debt of 5.9%, cost of equity of 9%, and a debt share of 60%.
CapEx	<ul style="list-style-type: none"> Supply CapEx (excluding installation) for mooring lines, anchors, and intra-array cables was derived from the design work in previous sections and design basis cost inputs. Project development costs were set to 9.7% of CapEx, following [1] Interest during construction was set at 5.9%, consistent with the recommended cost of debt in [1].
OpEx	<ul style="list-style-type: none"> Fixed O&M costs were derived from [26], as recommended in [1]. Updated estimates of \$46/kW were used, covering insurance, lease fees, operating facilities, training, onshore logistics, technical resources, and administrative support, replacing the outdated \$31/kW estimate in [1].

The costs shown in Table 16, Table 17, and Table 18 correspond to the system designs developed and discussed in earlier sections of the report. The mooring line and cable material costs are estimated based on [1]. The suction anchor costs shown in Table 17 reflect material and fabrication estimates only, based on indicative ranges reported in [1], and are included here solely for comparative purposes. The dynamic cable cost per meter in

Table 18 includes the cost of the buoyancy modules.

Table 16. Cost and Mass of the Mooring System

Mooring Cost/Line (USD)	Total Wind Farm Mooring Cost (USD)	Mooring Mass/Line (tonnes)
777,795	156,336,798	248.64

Table 17. Cost and Mass of the Suction Anchor

Anchor Cost (USD)	Total Wind Farm Anchor Cost (USD)	Anchor Mass (tonnes)
589953	118,580,453	133.17

Table 18. Cost and Mass of 66-kV Array Cables

Cable Conductor Area (mm ²)	Dynamic Cable Cost (USD/m)	Static Cable Cost (USD/m)	Dynamic Cable Total Length (m)	Static Cable Total Length (m)	Connector Cost/cable (USD)	Joint Cost/cable (USD)	# of Cable	Total Wind Farm Cable Cost (USD)	Total Wind Farm Cable Mass (kg)
300	540	500	156	884	203,000	237,000	80	77,294,400	3,050,112
630	714	655	156	884	273,000	237,000	48	57,619,056	2,783,539
1000	1043	959	156	-	352,000	237,000	6	4,510,206	70,200
630	714	655	-	23370	-	-	1	15,307,350	1 303,111
1000	1043	959	-	9575	-	-	1	9,182,425	718,125
Total								163,913,437	7,925,087

7.3 Results

This subsection presents the results for FCR, CapEx, OpEx, net AEP, and LCOE.

7.3.1 FCR

As discussed in Section 7.2.2, FCR estimates are primarily driven by inputs from [1] and calculated without adjustments for depreciation or taxes. Table 19 summarizes the parameters and resulting FCR outputs.

Table 19. Inputs and outputs used to derive FCR

Parameter	Units	Value
Project design life	years	25
Tax Rate (combined state and federal)	%	0%*
Inflation rate	%	2.5%
Debt fraction	%	60.0%
Debt interest rate (nominal)	%	5.9%
Return on equity (nominal)	%	9.0%
WACC (nominal; pre-tax)	%	7.14%
WACC (real; pre-tax)	%	4.53%
Capital recovery factor (nominal; pre-tax)	%	8.69%
Capital recovery factor (real; pre-tax)	%	6.76%
Depreciation adjustment (NPV)	%	100%*
Project finance factor	%	100%
FCR (nominal)	%	8.69%
FCR (real)	%	6.76%

*: Reflects the assumption that the Design Basis excludes tax and depreciation [1].

7.3.2 CapEx

Table 20 presents the CapEx breakdown from ORBIT, with the final column describing how each cost was modelled.

Table 20. CapEx Breakdown in 2024 USD

Component	Category	Value (\$/kW)	How was it modelled?
Turbine	Turbine	1,770	ORBIT input based on [21]
Substructure	BOS CapEx	1,244	ORBIT output
Substructure installation	BOS CapEx	264	ORBIT output
Mooring system	BOS CapEx	274	ORBIT input based on Section 7.2.2
Mooring system installation	BOS CapEx	47	ORBIT output, mass from Section 7.2.2
Array system	BOS CapEx	163	ORBIT input based on Section 7.2.2
Array system installation	BOS CapEx	224	ORBIT output
Offshore substation (OSS)	BOS CapEx	264	ORBIT output
OSS installation	BOS CapEx	7	ORBIT output
Export system	BOS CapEx	1125	ORBIT output
Export system installation	BOS CapEx	782	ORBIT output
Onshore substation	BOS CapEx	218	ORBIT output
Project development	BOS CapEx	886	ORBIT output
Commissioning	Soft CapEx	81	ORBIT output
Construction financing	Soft CapEx	704	ORBIT output
Construction insurance	Soft CapEx	162	ORBIT output
Decommissioning	Soft CapEx	265	ORBIT output
Procurement contingency	Soft CapEx	329	ORBIT output
Installation contingency	Soft CapEx	457	ORBIT output
Total	-	9,266	-

The resulting CapEx of \$9,266/kW (2024 USD) excludes potential grid/network upgrades as well as supply chain and port development costs. These costs may represent additional burdens in regions where network upgrades beyond the POI may not be financed by the transmission system operator, or in less mature markets where suppliers and port authorities may lack the long-term demand certainty to invest in infrastructure and manufacturing without developer support. These exclusions allow CapEx to remain directly comparable across designs in different regions, but they should be included when estimating the CapEx of an actual project.

7.3.3 OpEx

Table 21 summarizes the OpEx breakdown derived from WOMBAT, with the final column describing how each cost was modelled.

Table 21. OpEx Breakdown in 2024 USD

Component	Category	Value (\$/kW-year)	How was it modelled?
Labor (technicians)	Maintenance	5.9	WOMBAT input based on assumed # of year-round full-time technicians
Materials	Maintenance	2.0	WOMBAT output
Equipment (vessels)	Maintenance	8.41	WOMBAT output
AHT	Maintenance	3.23	WOMBAT output
CTV 1	Maintenance	1.39	WOMBAT output
CTV 2	Maintenance	1.39	WOMBAT output
CTV 3	Maintenance	1.39	WOMBAT output
DSV	Maintenance	1.0	WOMBAT output
Port fees	Operations	25.0	WOMBAT input based on repair time at port and monthly port fee from [22]
Insurance	Operations	31.0	WOMBAT input from [26]
Total	-	72.31	-

AHT = anchor handling tug; CLV = cable lay vessel; CTV = crew transfer vessel; DSV = diving support vessel.

7.3.4 Net AEP

Table 22 presents the loss breakdown from WAVES, showing how the net capacity factor was derived from the gross capacity factor calculated in FLORIS.

Table 22. Breakdown of Losses from Gross to Net Generation

Parameter	Units	Value	How was it modelled?
Gross capacity factor	%	66.15%	FLORIS output
Total losses	%	14.5%	WAVES output
Availability losses	%	3.9%	WOMBAT output, production-based
Electrical losses	%	4.0%	WAVES output based on cable distance
Environmental losses	%	1.6%	WAVES default input
Technical losses	%	1.2%	WAVES default input
Wake losses (internal)	%	4.7%	FLORIS output
Net capacity factor	%	56.5%	WAVES output
Net AEP per kW	MWh/kW	4.955	WAVES output

7.3.5 LCOE

Figure 27 presents the LCOE breakdown for all CapEx and OpEx components, incorporating financing assumptions and net AEP. The resulting LCOE of \$138.01/MWh (real 2024 USD) excludes potential grid/network upgrades, as well as supply chain and port development costs that may be required in less mature markets. These exclusions ensure that the LCOE remains directly comparable to other designs in different regions, but they should not be omitted when calculating the LCOE of an actual project.

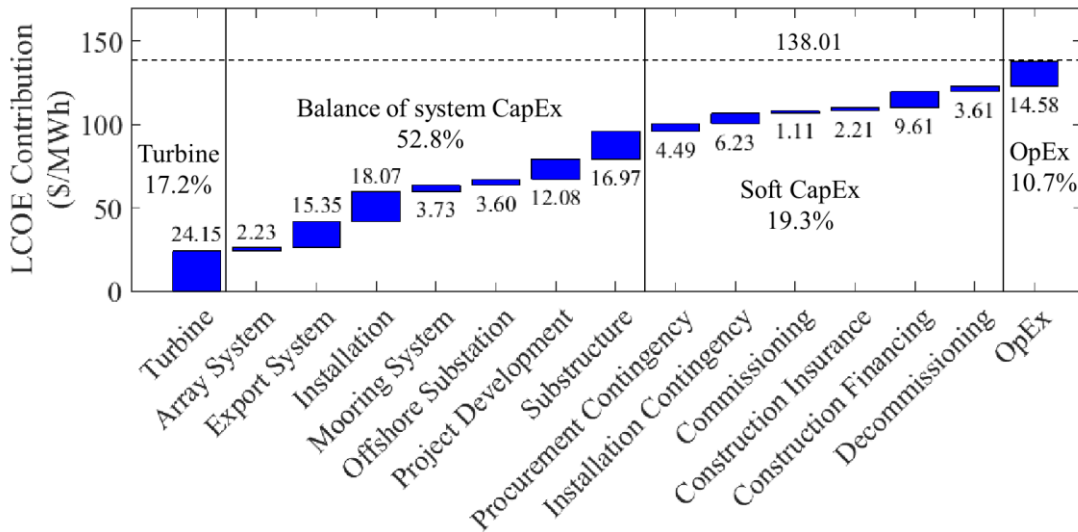


Figure 27. LCOE waterfall in \$/MWh.

8 Conclusion

In this report, the IEA Wind RFA1 reference shallow-water floating wind array design is presented as a baseline for future floating wind research. Consistent across the design subgroups, the reference concept adopts a 1-GW wind farm composed of the IEA Wind 15-MW reference wind turbine mounted on the VoltturnUS-S semisubmersible platform. The mooring system and dynamic cable are specifically designed for the Sørliche Nordsjø II site, with a representative water depth of 60 m.

The mooring system adopts a semi-taut chain–polyester–chain configuration, with clump weights and subsea buoys strategically positioned to reduce peak mooring tensions and prevent seabed abrasion. Dynamic simulations are conducted to evaluate the performance of the mooring system and dynamic cable under extreme environmental conditions. The results show that the mooring system satisfies the ULS criteria while avoiding slack-line events and seabed contact of the polyester segment. For FLS assessment, simulations based on fatigue bins representative of the metocean conditions at SN2 over a 25-year service life demonstrate that the fatigue criteria are also satisfied. The dynamic cable adopts a lazy-wave configuration and is modelled using a conductor cross-sectional area of 630 mm². Both ULS and FLS evaluations are performed, and the resulting maximum tension and curvature remain within the allowable limits.

The reference wind farm adopts a rectangular grid layout with uniform spacing between adjacent turbines in both row and column directions. The electrical system consists of a single OSS, with inter-array cables sized according to the number of downstream turbines connected in series. Cable routing is designed to avoid interference with the mooring system.

The cost and logistics modelling evaluates the economic performance of the reference shallow-water floating wind farm while accounting for the specific mooring, cable, and array layout characteristics. Process-based installation and O&M logistics models are combined with wake-loss and AEP simulations to estimate CapEx, OpEx, energy generation, and key financial metrics. The resulting LCOE for the 1-GW floating wind farm is estimated at \$138.01/MWh, providing a representative benchmark for assessing alternative floating wind array designs.

The design files, including a YAML-based description of the full array in the Task 49 ontology format, simulation input files for the mooring system and dynamic cable designs, and cost model input files, have been made publicly available in a dedicated repository under the IEA Wind Task 49 GitHub organization [27].

Overall, the proposed reference design provides a baseline framework for future studies on floating wind arrays in shallow to intermediate water depths. The detailed mooring, cable, and array design information presented in this report can be directly adopted or further refined in subsequent research. In addition, the techno-economic results establish a benchmark against which alternative floating wind farm configurations and design strategies may be evaluated.

References

- [1] Hall, M., E. Lozon, F. Devoy McAuliffe, M. Baudino Bessone, I. Bayati, M. Bowie, P. Bozonnet, et al. 2024. *The IEA Wind Task 49 Reference Floating Wind Array Design Basis*. Golden, CO: National Renewable Energy Laboratory. NREL/TP-5000-89709. <https://docs.nrel.gov/docs/fy24osti/89709.pdf>.
- [2] Gaertner, E., J. Rinker, L. Sethuraman, F. Zahle, B. Anderson, G. Barter, N. Abbas, et al. 2020. *Definition of the IEA 15-Megawatt Offshore Reference Wind Turbine*. Golden, CO: National Renewable Energy Laboratory. NREL/TP-5000-75698. <https://docs.nrel.gov/docs/fy20osti/75698.pdf>.
- [3] Allen, C., A. Viselli, H. Dagher, A. Goupee, E. Gaertner, N. Abbas, M. Hall, and G. Barter. 2020. *Definition of the UMaine VoltturnUS-S Reference Platform Developed for the IEA Wind 15-Megawatt Offshore Reference Wind Turbine*. Golden, CO: National Renewable Energy Laboratory. NREL/TP-5000-76773. <https://docs.nrel.gov/docs/fy20osti/76773.pdf>.
- [4] Cheynet, E., Li, L., and Jiang, Z. 2024. “Metocean Conditions at Two Norwegian Sites for Development of Offshore Wind Energy.” *Renewable Energy* 224: 120184. <https://doi.org/10.1016/j.renene.2024.120184>.
- [5] Haakenstad, H., and Ø. Breivik. 2022. “NORA3. Part II: Precipitation and Temperature Statistics in Complex Terrain Modeled with a Nonhydrostatic Model.” *Journal of Applied Meteorology and Climatology* 61 (10): 1549–1572. <https://doi.org/10.1175/JAMC-D-22-0005.1>.
- [6] Creane, S., P. Santos, K. Kölle, D. Airoidi, M. Bakhoday-Paskyabi, M. Biglu, W. Brown, et al. 2024. *Reference Site Conditions for Floating Wind Arrays*. Golden, CO: National Renewable Energy Laboratory. NREL/TP-5000-89937. <https://docs.nrel.gov/docs/fy24osti/89937.pdf>.
- [7] Lee, C. F., S. Fjermedal, and M. C. Ong. 2025. “Design and Comparative Analysis of Mooring Systems for a Combined Wind and Wave Energy System at Intermediate Water Depth.” *Journal of Ocean Engineering and Science* 10 (4): 492–508. <https://doi.org/10.1016/j.joes.2024.11.002>.
- [8] American Bureau of Shipping (ABS). 2020. *Guide for Building and Classing Floating Offshore Wind Turbines*. Spring, TX: American Bureau of Shipping. <https://ww2.eagle.org/content/dam/eagle/rules-and-guides/current/offshore/fowt-guide-july20.pdf>.
- [9] DNV. 2021. DNV-OS-E301: “Position Mooring.” Available from dnv.com.
- [10] SINTEF. 2026. *SIMA Documentation, Version 5.0*. Accessed May 11, 2026. <https://sima.sintef.no/docs/5.0/sima/index.html>.
- [11] Xu, K., Larsen, K., Shao, Y., Zhang, M., Gao, Z., and Moan, T. 2021. “Design and Comparative Analysis of Alternative Mooring Systems for Floating Wind Turbines in Shallow Water with Emphasis on Ultimate Limit State Design.” *Ocean Engineering* 219: 108377. <https://doi.org/10.1016/j.oceaneng.2020.108377>.

- [12] Bridon Bekaert. 2013. *Advanced Rope Solutions for the Offshore Oil and Gas Exploration, Construction and Production Industries*. Product catalogue. Bridon Bekaert.
- [13] Falkenberg, E., Åhjem, V., and Yang, L. 2017. “Best Practice for Analysis of Polyester Rope Mooring Systems.” In *Proceedings of the Offshore Technology Conference 2017*. Houston, TX: Offshore Technology Conference. <https://doi.org/10.4043/27761-MS>.
- [14] Miner, M. A. 1945. “Cumulative Damage in Fatigue.” *Journal of Applied Mechanics* 12 (3): A159–A164. <https://doi.org/10.1115/1.4009458>.
- [15] DNV. 2013. *DNV-OS-E301 Position Mooring*. Offshore Standard. Høvik, Norway: Det Norske Veritas.
- [16] Aubeny, C.P., Han, S.W., and Murff, J. D. 2003. “Inclined Load Capacity of Suction Caissons.” *International Journal for Numerical and Analytical Methods in Geomechanics* 27(14): 1235–1254. <https://doi.org/10.1002/nag.319>.
- [17] American Petroleum Institute (API). 2005. APO RP 2SK: “Design and Analysis of Stationkeeping Systems for Floating Structures.
- [18] Janocha, M. J., Ong, M. C., Lee, C. F., Chen, K., and Ye, N. 2024. “Reference Power Cable Models for Floating Offshore Wind Applications.” *Sustainability* 16 (7): 2899. <https://doi.org/10.3390/su16072899>.
- [19] Norwegian Ministry of Energy. 2023. *Appendix 3: The Project Area, Grid Connection and Regulatory Conditions for the First Phase of Sørilige Nordsjø II*. Oslo, Norway: Norwegian Government.
- [20] National Laboratory of the Rockies. 2024. “Annual Technology Baseline – Financial Cases and Methods.” https://atb.nrel.gov/electricity/2024/financial_cases_&_methods.
- [21] Stehly, T., Duffy, P., and Mulas Hernando, D. 2024. “Cost of Wind Energy Review: 2024 Edition.” National Renewable Energy Laboratory. NREL/PR-5000-91775. <https://www.osti.gov/servlets/purl/2479271/>.
- [22] National Laboratory of the Rockies. No date. “Offshore Renewable Balance-of-system Installation Tool (ORBIT).” <https://github.com/NLRWindSystems/ORBIT>.
- [23] National Laboratory of the Rockies. No date. “Windfarm Operations & Maintenance cost-Benefit Analysis Tool.” <https://github.com/NLRWindSystems/WOMBAT>.
- [24] National Laboratory of the Rockies. No date. “FLORIS.” <https://github.com/NatLabRockies/floris>.
- [25] National Laboratory of the Rockies. No date. “Wind Asset Value Estimation System.” <https://github.com/NatLabRockies/WAVES>.

[26] BVG Associates. No Date. “Wind Farm Costs.” In *Guide to a Floating Offshore Wind Farm*. <https://guidetofloatingoffshorewind.com/wind-farm-costs/>.

[27] Ong, M.C., Lee, C.F., Mulas Hernando, D., Janocha, M.J., Feng, J., 2026. “IEA Wind Task 49 Shallow Water Array Design”. <https://doi.org/10.5281/zenodo.20290990>